Available online at www.sciencedirect.com

SCIENCE DIRECT®

International Journal of Mass Spectrometry 235 (2004) 223–228

International Journal of Mass Spectrometry

www.elsevier.com/locate/ijms

Electron-impact ionisation cross-sections of the $CClF_3$ and CCl_3F molecules

Borja Sierra [a], Roberto Martínez [b], Carolina Redondo [a], Fernando Castaño [a,*]

[a] *Facultad de Ciencias, Departamento de Química Física, Universidad del País Vasco, Apdo. 644, 48080 Bilbao, Spain*
[b] *Facultad de Farmacia, Departamento de Química Física, Universidad del País Vasco, Paseo de la Universidad, 7, 01006 Vitoria, Spain*

Received 7 April 2004; accepted 21 May 2004

Abstract

An investigation is reported on the absolute partial ionisation cross-sections of the set of ions lay down following the collisions of electrons with $CClF_3$ and CCl_3F molecules. Experiments were carried out in a pulsed supersonic expansion inside a time-of-flight mass spectrometer. The electron kinetic energies used were in the 10–100 eV range and the electron and molecular beams arranged to cross at right angle. CF_3^+ ions for the $CClF_3$ parent molecule and CCl_2F^+ for the CCl_3F are the fragments with highest ionisation cross-sections (ICS). $CClF_2^{2+}$ and CF_3^{2+} dications are observed in the dissociative ionisation of $CClF_3$ and their contribution to the total ionisation cross-sections is just over 1%; in the case of the CCl_3F molecule only the CCl_2F^{2+} double ion appears and its ionisation cross-section is even smaller than those produced by electron impact on $CClF_3$.

Keywords: Dissociative ionisation; Dissociative ionisation partial cross-sections; Electron impact ionisation; Chlorofluoromethanes dissociative ionisation

1. Introduction

The knowledge of the electron-impact partial ionisation cross-sections (ICS) and dissociative pathways of molecules is crucial to model, control and optimise the properties of a variety of industrial and other plasmas [1]. Partial ICSs play a fundamental role in choosing the appropriate conditions to attain the highest concentrations of active species for etching and deposition. Christophorou and Olthoff [2] have assessed and compiled the available data on the interactions of low-energy electrons (for the most part, below 100 eV) with molecules of interest in plasma processing and atmospheric chemistry.

Chlorofluoromethanes are a standard choice to create fast reactive etching species in semiconductor processing plasmas or for chemical vapour deposition [3]. Furthermore, the title molecules $CClF_3$ (CFC-13) and CCl_3F (CFC-11) have a notorious influence on the chemistry of the upper atmosphere. In particular, they have a global warming potential (GWP) rated several orders of magnitude higher than that of the paradigmatic CO_2 molecule [4]. Their photolysis in the upper atmosphere yields Cl atoms, an efficient depleting agent of stratospheric ozone [5]. Light emission following electron-impact on $CClF_3$ and CCl_3F has been reported by van Sprang and Brogersma [6], showing that the CCl^+ (A) and its transition to the ground state is responsible for the broad emissions observed in the 200–400 nm region. Electron-impact on CCl_3F has also been employed in the laboratory to yield sizeable concentrations of free radicals and ions in excited states that are further used as reactants in subsequent reactions as well as to measure radiative lifetimes [7,8] of species which are difficult to obtain by other methods. Total inelastic scattering cross-sections of $CClF_3$ and CCl_3F have been studied [9] in order to test the additivity rules and complex optical potentials. Electron energy-loss spectroscopy of chlorofluoromethanes and their Rydberg states have also been reported [10].

Measurements of the electron-impact total ICSs for the CF_3Cl employing the total ion current method have been presented by Bart et al. [11] in an extensive study on perfluorinated hydrocarbons and small halocarbons. The work also discusses the additivity of the bond contributions to the ICS maximum. A study of the total ICS of $CClF_3$ and CCl_3F at three electron energies (20, 35 and

---

* Corresponding author. Tel.: +34 94 601 2533; fax: +34 94 464 8500.
E-mail address: qfpcaalf@lg.ehu.es (F. Castaño).

1387-3806/$ – see front matter © 2004 Elsevier B.V. All rights reserved.
doi:10.1016/j.ijms.2004.05.009

70 eV) along with 62 other hydrocarbons, fluorocarbons and halogen-substituted hydrocarbons has been presented by Beran and Kevan [12]. The wide interest in experimental ICS is supported by a rising interest in theoretical models to compute total ICS. Experimental total ICSs of the CCl_xF_{4-x} ($x = 1$–4) and the computed theoretical results have been discussed elsewhere [13]. Partial and total ICS, dissociative ionisation and temperature-dependent attachment of the nearby CCl_2F_2 molecule have been reviewed and discussed recently [14–16]. Partial ICS of CF_3Br and CF_3I fluoromethanes have been reported by Jiao et al. [17]. The present work reports a detailed experimental study of the electron-impact absolute partial ICS of both $CClF_3$ and CCl_3F molecules in the electron energy range from the ionisation threshold up to 100 eV.

2. Experimental

A detailed description of the experimental set-up and the method used to measure partial ICS has been presented elsewhere [18] and only a succinct account is given below. Before the experiment, both reference and target gases are stored in a stainless steel cylinder at a pressure of 3 bar (MKS-baratron 750B, 1% accuracy). Dissociative ionisation is produced by spatial and temporal crossing of a well-characterized kinetic energy (0.5 eV FWHM) pulsed electron beam with a supersonic expansion of a mixture of a noble gas (Ar, reference) seeded either with $CClF_3$ or CCl_3F. The collisions take place in the scattering region of a Wiley–McLaren style lineal double focusing time-of-flight mass spectrometer (TOF-MS) [19]. After the collisions the ions are extracted by pulsing the repeller grid of the TOF-MS to 200 V and then accelerated by a second stronger electric field into the TOF drift tube and finally onto the multichannel plate (MCP, C-07001, 18 mm diameter) detector. The focusing of the ions on the detector is aided by electrostatic lenses and the generated signals are amplified and routed to a digital oscilloscope and to a PC for further study and storage.

Absolute partial ICSs are attained by comparing the signal intensities of the target ion under study and that of a reference gas (e.g., Ne^+ (20.2 amu), Ar^+ (40.0 amu) or Kr^+ (83.8 amu)) [20]. The method benefits from the simultaneous measurement of target and reference gases, and fluctuations in electron energy or intensity affect both gases equally. As a result, the accuracy is limited by that of the reference data.

The mass spectra bands of the ion fragments containing chlorine atoms are split, as expected from the presence of the ^{35}Cl and ^{37}Cl isotopes. The ratio of their areas is close to 3:1, in accord with the relative isotope abundance. The total partial ICSs is computed by integrating the area under the bands of both isotopes and comparing with that of the reference gas.

Errors stem mainly from the uncertainties of reference gas ICSs (3–5% for Ne^+, Ar^+ and Kr^+ [20]), the pressure inaccuracies (1% for $CClF_3$, 2–3% for mixtures CCl_3F/Ar, Kr), the percentage of ions reaching the detector and the single ion counting efficiency of the MCP detector. The effects due to the focusing of ions are larger for light ions (10–15%), since their higher velocities and broad kinetic energy distributions (KEDs) preclude their complete collection. For a selected species, the errors are usually larger near the onset of the cross-section, because of the uncertainties in the electron energy at low voltages. Partial ICS were obtained as a result of at least five different runs.

$CClF_3$ from Union Carbide (98% purity), CCl_3F from Sigma-Aldrich (purity >99%) and high purity Ar, Kr and Ne from Praxair were used without further purification.

3. Results and discussion

A considerable number of charged fragments are observed in the collisions of 10–100 eV electrons with $CClF_3$, including $CClF_n^+$ ($n = 1$–3), CF_n^+ ($n = 1$–3), CCl^+, the atomic

Table 1
Partial and total ionisation cross-sections of ions produced by electron-impact on $CClF_3$

Energy (eV)	CF_3^+	$CClF_2^+$	Cl^+	CF_2^+	CF^+	C^+	CCl^+	F^+	$CClF_3^+$	$CClF^+$	$CClF_2^{2+}$	CF_3^{2+}	Total
20	1.246	0.259	0.034	0.0529	0.011	–	0.003	–	0.040	–	–	–	1.646
25	1.765	0.387	0.078	0.123	0.035	–	0.003	–	0.042	0.009	–	–	2.442
30	2.591	0.652	0.182	0.262	0.104	0.003	0.013	–	0.047	0.013	–	–	3.867
35	2.944	0.859	0.324	0.364	0.208	0.011	0.018	0.008	0.048	0.014	0.018	–	4.799
40	3.146	1.000	0.407	0.412	0.271	0.025	0.053	0.011	0.054	0.015	0.026	0.001	5.421
45	3.252	1.109	0.501	0.460	0.301	0.047	0.074	0.025	0.060	0.018	0.039	0.007	5.893
50	3.346	1.180	0.563	0.493	0.307	0.062	0.077	0.037	0.062	0.022	0.048	0.009	6.206
55	3.390	1.257	0.624	0.523	0.321	0.076	0.079	0.051	0.060	0.018	0.062	0.014	6.475
60	3.426	1.277	0.630	0.545	0.336	0.081	0.077	0.059	0.060	0.020	0.069	0.021	6.601
65	3.380	1.317	0.653	0.558	0.331	0.084	0.083	0.066	0.057	0.024	0.075	0.021	6.649
70	3.433	1.365	0.709	0.577	0.347	0.094	0.085	0.068	0.066	0.024	0.079	0.023	6.870
75	3.452	1.396	0.729	0.605	0.350	0.107	0.089	0.073	0.060	0.026	0.081	0.026	6.994
80	3.446	1.412	0.759	0.611	0.352	0.108	0.104	0.078	0.057	0.025	0.084	0.026	7.063
85	3.434	1.439	0.742	0.623	0.352	0.121	0.091	0.088	0.066	0.026	0.090	0.026	7.098

Cross-sections are in 10^{-20} m^2 units.

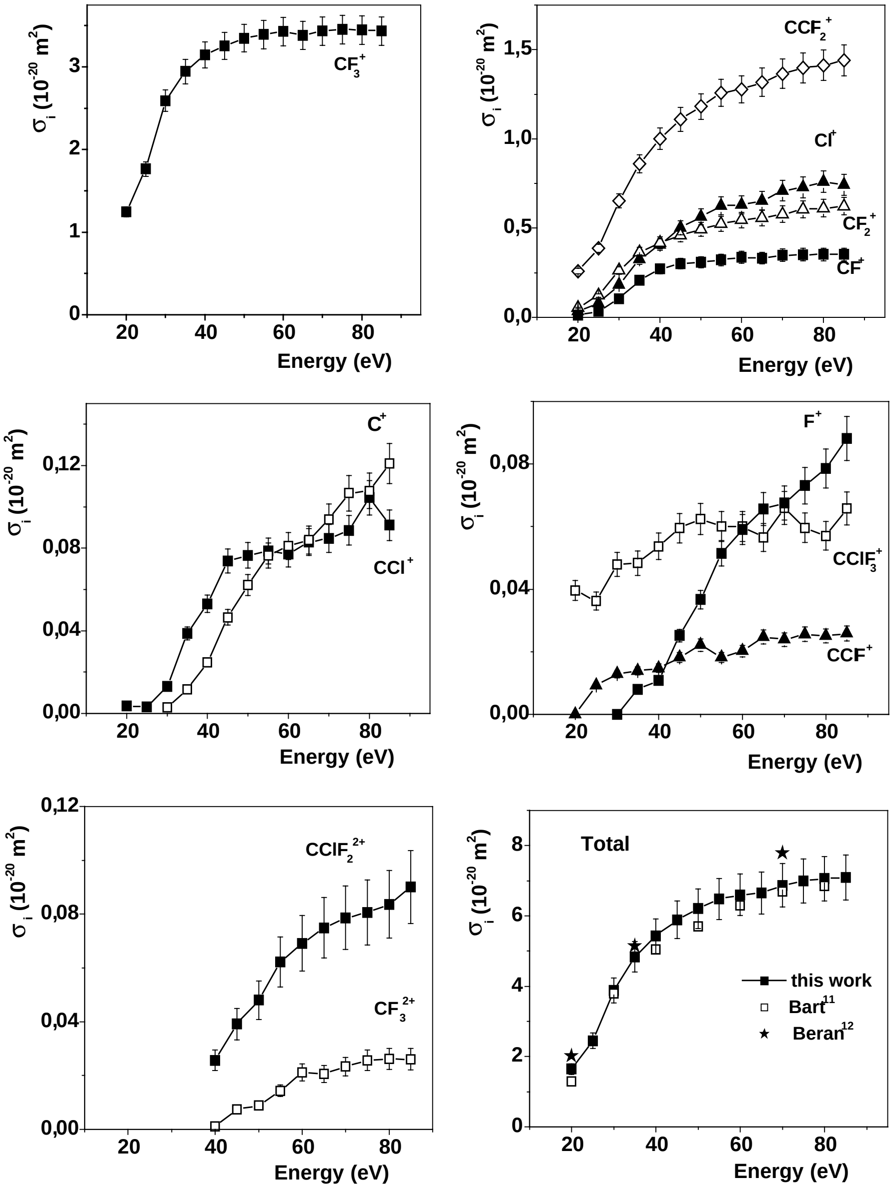

Fig. 1. Partial ionisation cross-sections (ICSs) of $CF_3{}^+$, $CClF_2{}^+$, Cl^+, $CF_2{}^+$, CF^+, C^+, CCl^+, F^+, $CClF_3{}^+$, $CClF^+$, $CClF_2{}^{2+}$ and $CF_3{}^{2+}$ produced by electron-impact on $CClF_3$. The electron kinetic energy varies from threshold to near 100 eV. The last figure shows the total ICSs and earlier experimental data. (□) Bart et al. [11]; (★) Beran and Kevan [12].

ions C^+, F^+ and Cl^+, and the doubly charged ions $CClF_2{}^{2+}$, $CF_3{}^{2+}$. The detailed experimental partial ICS profiles as a function of electron energy are plotted in Fig. 1. The total ICS is also included as well as the previously reported experimental results. A comparison between the experimental and theoretical total ICS has been presented recently [13]. For convenience the numerical partial ICS are given in Table 1.

The ICS of the $CClF_3$ parent ion is relatively small. It increases rapidly for electron energies just above threshold followed by a levelling off to about $5 \times 10^{-22}\,m^2$ at higher energies (Fig. 1). Ion production yield is very close to that for $CBrF_3$ [17]. In the chlorofluoromethane family, it is found that the higher the number of fluorine atoms in the molecule, the more stable is the parent ion. In fact, from our results and others [15] one may state that the stability sequence is $\sigma_{CClF_3{}^+} > \sigma_{CCl_2F_2{}^+} > \sigma_{CCl_3F^+} \approx 0$ (not observed). The appearance of the parent ion seems to be related to the electronic excitation of the precursor either to a repulsive state or to a state with a shorter lifetime than that of the time-of-flight in the mass spectrometer [21].

It is worth noting that the partial ICS maxima of the ions from $CClF_3$ molecule varies considerably, from 3.5 to 0.02 $\times 10^{-20}\,m^2$. The ion produced with the highest efficiency is $CF_3{}^+$ accompanied by the atom bonded with less energy (Cl) as apparent from appearance energy measurements [22]. Its partial ICS is close to that of the sum of all other ions. It is readily observed that the magnitude of the ICS of the fluorocarbon ions follows an ordering $\sigma_{CF_3^+} > \sigma_{CF_2^+} > \sigma_{CF^+}$ in the electron energy range studied. This behaviour may be justified as if the CF_3^+ ion were ejected by dissociative ionisation from the ion parent molecule with a large kinetic energy excess, that is further redistributed among the ion bonds, producing dissociation to a fluorine atom and a CF_2^+ ion. A similarly process leads to CF^+ ion. The discussion of the ions appearance potentials and their released kinetic energy has been shown to be useful for the study of the dissociative ionisation energy balance [16,22].

$CClF_2^+$, $CClF^+$ or CCl^+ heavy ions are released in the dissociative ionisation of $CClF_3$ (Fig. 1), but also in that of CCl_2F_2 [15] and the pattern of the ICSs is similar. In fact, at electron energies of 80–90 eV, the lower the total bonding energies of the partner atom or atoms lost, the higher the ICS maximum. Furthermore, in the CCl_3F, CCl_2F_2 and $CClF_3$ series, the ICSs maxima of the $CClF^+$ ion decreases steadily from 0.9 to 0.02 × 10^{-20} m^2, since the bonding energy of the C–Cl bond is lower than that of C–F.

$CClF_2^{2+}$ and CF_3^{2+} dications are easily detected in the electron–$CClF_3$ collisions. Their joint ICS contributions have a steady increase in the 40–80 eV range and at 80 eV reach 0.10 × 10^{-20} m^2, i.e., only 1.4% of the total ICS. The ratio is smaller than that reported for the HCl/HCl^{2+} system, where for an ionisation threshold of the same order, the contribution attains 12% at 100 eV (3% at 50 eV). The issue of instability of doubly charged ions is of renewed interest [23]. In the case of electron impact on CCl_3F only the CCl_2F^{2+} dication is observed, and its ICS contribution to the total ICS is less than 0.7%. Partial ICSs profile for

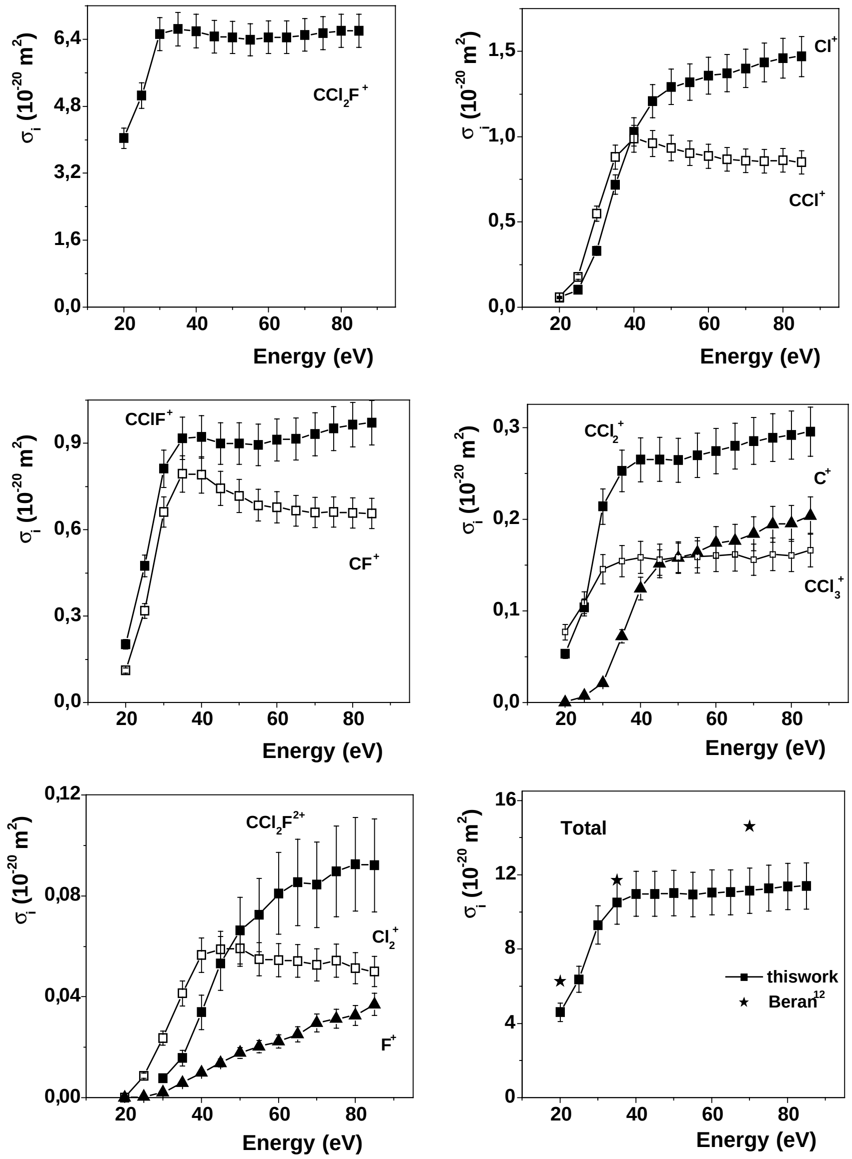

Fig. 2. Partial ionisation cross-sections (ICSs) of CCl_2F^+, Cl^+, CCl^+, $CClF^+$, CF^+, CCl_2^+, C^+, CCl_3^+, Cl_2^+, F^+ and CCl_2F^{2+}, produced by electron-impact on CCl_3F. The electron kinetic energy varies from threshold to near 100 eV. The last figure shows the total ICSs and earlier experimental data. (★) Beran and Kevan [12].

Table 2
Partial and total ionisation cross-sections of ions produced by electron-impact on CCl_3F

Energy (eV)	CCl_2F^+	Cl^+	CCl^+	$CClF^+$	CF^+	$CCl_2{}^+$	C^+	$CCl_3{}^+$	CCl_2F^{2+}	$Cl_2{}^+$	F^+	Total
20	4.037	0.055	0.058	0.202	0.111	0.0529	–	0.077	–	–	–	4.592
25	5.057	0.103	0.176	0.474	0.318	0.103	0.007	0.109	–	0.009	–	6.356
30	6.524	0.331	0.549	0.811	0.661	0.214	0.021	0.145	0.008	0.024	0.002	9.289
35	6.642	0.718	0.879	0.917	0.793	0.252	0.072	0.154	0.016	0.041	0.006	10.491
40	6.596	1.027	0.988	0.921	0.790	0.265	0.124	0.158	0.034	0.056	0.010	10.970
45	6.461	1.207	0.960	0.899	0.743	0.265	0.151	0.156	0.053	0.058	0.014	10.968
50	6.445	1.291	0.934	0.899	0.717	0.264	0.158	0.158	0.066	0.059	0.018	11.001
55	6.388	1.319	0.903	0.894	0.685	0.269	0.163	0.159	0.072	0.055	0.020	10.928
60	6.449	1.357	0.885	0.912	0.677	0.275	0.174	0.160	0.081	0.055	0.022	11.046
65	6.449	1.371	0.867	0.915	0.665	0.279	0.176	0.161	0.085	0.054	0.025	11.049
70	6.503	1.399	0.858	0.932	0.659	0.285	0.184	0.155	0.084	0.053	0.029	11.143
75	6.549	1.434	0.856	0.951	0.661	0.289	0.194	0.161	0.089	0.054	0.031	11.271
80	6.605	1.458	0.861	0.964	0.658	0.292	0.195	0.160	0.092	0.051	0.033	11.371
85	6.597	1.469	0.849	0.971	0.656	0.295	0.204	0.166	0.092	0.050	0.037	11.386

Cross-sections are in $10^{-20}\,m^2$ units.

the CCl_2F^{2+} dication has uncertainties estimated to be in the 15–20% range.

The partial ICS profiles of the charged fragments originating in the electron–CCl_3F collision are depicted in Fig. 2 and include $CCl_3{}^+$, CCl_2F^+, $CClF^+$, $CCl_2{}^+$, CCl^+, CF^+, $Cl_2{}^+$ the atomic ions C^+, F^+ and Cl^+, and the CCl_2F^{2+} dication. The figure also includes the total ICS, and is compared with the few existing reported experimental results [12]. Quantitative ICS are summarised in Table 2. It should be noted that the parent ion CCl_3F^+ is not observed at all and the CCl_2F^+ ion is produced with the highest ICS. In addition, the Cl^+ partial ICS from CCl_3F at any electron energy is nearly twice as large as that of $CClF_3$, suggesting an ionisation mechanism leading preferentially to the production of Cl^+. However, a striking contrast can be noted in the ICSs behaviour of the $CCl_n{}^+$ ($n = 1$–3) series from CCl_3F compared with $CF_n{}^+$ ($n = 1$–3) from $CClF_3$. The ICS of the ions derived from CCl_3F follows the sequence $\sigma_{CCl^+} > \sigma_{CCl_2{}^+} > \sigma_{CCl_3{}^+}$, exactly opposite to that for $CClF_3$, namely $\sigma_{CF^+} < \sigma_{CF_2{}^+} < \sigma_{CF_3{}^+}$. The discrepancy may be justified in terms of the larger dissociation effects in the parent-ion energy redistribution. It may well happen that the electronic states accessible by Franck–Condon transitions are above the thermodynamic threshold for bond dissociation. As a consequence, dissociative ionisations proceed through channels where the excess energy is distributed among the fragments resulting in a larger fragmentation.

4. Conclusions

This work reports a mass selective study of the partial ICSs of the ions produced by electron collisions with $CClF_3$ and CCl_3F molecules. The electron energies range from ionisation threshold to 100 eV. A comparative analysis of the mechanisms for formation of ions in $CClF_3$ and CCl_3F shows similarities and striking differences. In particular, the sequence of ICSs in the $CF_n{}^+$ ($n = 1$–3) and $CCl_n{}^+$ ($n = 1$–3) series is opposite, an effect that seems to be related to the accessible electronic states in Franck–Condon vertical transitions. $CClF_2{}^{2+}$ and $CF_3{}^{2+}$ double ions have been observed in the dissociative ionisation of $CClF_3$ but their contribution to the total ICS is very small (just over 1%); CCl_2F^{2+} ions appear in the dissociative ionisation of CCl_3F with an even smaller contribution to the total ICS.

Acknowledgements

The authors are grateful to MCYT (Madrid) for partial support of this work through Grant No. 2001-0511; to GV (Vitoria) and to UPV for a Consolidate Research Group Grant (2001-5). BS thanks MEC (Madrid) for a graduate fellowship associate to project 2001-0511.

References

[1] L.G. Christophorou, J.K. Olthoff, Fundamental Electron Interactions with Plasma Processing Gases, Kluwer Academic/Plenum, 2004.
[2] L.G. Christophorou, J.K. Olthoff, Appl. Surf. Sci. 192 (2002) 309, see also the databases and other information offered in the web of the NIST: http://webbook.nist.gov.
[3] K.H. Becker, in: H. Ehrhardt, L.A. Morgan (Eds.), Electron Collisions with Molecules, Clusters, and Surfaces, Plenum Press, New York, 1994, p. 127.
[4] J.H. Seinfeld, S.N. Pandis, in: Atmospheric Chemistry and Physics. From Air Pollution to Climate Change, Wiley Inc., 1998, p. 87.
[5] M.J. Molina, F.S. Rowland, Nature 249 (1974) 810.
[6] H.A. van Sprang, H.H. Brogersma, Chem. Phys. 35 (1978) 51.
[7] I. Tokue, T. Honda, Y. Ito, Chem. Phys. 140 (1990) 157.
[8] M. Kusakabe, Y. Ito, I. Tokue, Chem. Phys. 170 (1993) 243.
[9] Y. Jiang, J. Sun, L. Wan, Phys. Rev. A 52 (1995) 398.
[10] G.C. King, J.W. McConkey, J. Phys. B: At., Mol. Opt. Phys. 11 (1978) 1861.
[11] M. Bart, P.W. Harland, J.E. Hudson, C. Vallance, Phys. Chem. Chem. Phys. 3 (2001) 800.
[12] J.A. Beran, L. Kevan, J. Phys. Chem. 73 (1969) 3866.

[13] R. Martínez, B. Sierra, F. Castaño, J. Chem. Phys., submitted for publication.

[14] L.G. Christophorou, J.K. Olthoff, Y. Wang, J. Phys. Chem. Ref. Data 26 (1997) 1205.

[15] B. Sierra, R. Martínez, F. Castaño, Int. J. Mass Spectrom. 225 (2003) 127.

[16] B. Sierra, R. Martínez, F. Castaño, J. Phys. B: At., Mol. Opt. Phys. 37 (2004) 295.

[17] C.Q. Jiao, B. Ganguly, C.A.A. DeJoseph Jr., A. Garscadden, Int. J. Mass Spectrom. 208 (2001) 127.

[18] I. Torres, R. Martínez, M.N. Sánchez Rayo, F. Castaño, J. Phys. B: At., Mol. Opt. Phys. 33 (2000) 3615.

[19] W.C. Wiley, I.H. McLaren, Rev. Sci. Instrum. 26 (1955) 1150.

[20] R. Rejoub, B.G. Lindsay, R.F. Stebbings, Phys. Rev. A 65 (2002) 042713.

[21] H. Deutsch, K. Leiter, T.D. Märk, Int. J. Mass Spectrom. Ion Processes 67 (1985) 191.

[22] B. Sierra, R. Martínez, F. Castaño, in preparation.

[23] S. Harper, P. Calandra, S.D. Price, Phys. Chem. Chem. Phys. 3 (2001) 741.